Chapter 14
Gas Lasers

A gas laser contains atoms or molecules. Stimulated transitions occur in atoms between electronic states and in molecules between rotational, vibrational or electronic states. We describe various gas discharge lasers: helium–neon laser; metal vapor laser; argon ion laser; excimer laser; nitrogen laser; CO_2 laser; and optically pumped gas lasers.

The excimer laser and the CO_2 laser are two important industrial lasers. The excimer laser generates intense UV radiation pulses. The CO_2 laser is a source of infrared radiation. It has a high efficiency of conversion of electric power to power of laser radiation. The CO_2 laser is very versatile—it operates as continuous wave laser or as pulsed laser. Optically pumped gas lasers (pumped with CO_2 laser radiation) are suitable for generation of far infrared radiation.

We first treat two line broadening mechanisms that play a role in gas lasers: the Doppler and the collision broadening. Then we discuss different gas lasers.

14.1 Doppler Broadening of Spectral Lines

Doppler broadening is a main broadening mechanism of spectral lines for gases at low pressure. The frequency of the radiation that is due to transitions between two discrete energy levels of an atom (or a molecule) is

$$\nu = \nu_0 + (\mathrm{v}_z/c)\,\nu_0, \tag{14.1}$$

where ν_0 is the frequency of the radiation emitted by the atom at rest and v_z is the velocity component in z direction. The atoms in a gas have a Maxwellian velocity distribution

$$f(\mathrm{v}_x, \mathrm{v}_y, \mathrm{v}_z) = \left(\frac{m}{2\pi kT}\right)^{3/2} \exp\left(-\frac{m}{2kT}(\mathrm{v}_x^2 + \mathrm{v}_y^2 + \mathrm{v}_z^2)\right). \tag{14.2}$$

K.F. Renk, *Basics of Laser Physics*, Graduate Texts in Physics,
DOI 10.1007/978-3-319-50651-7_14

T is the temperature of the gas, m the mass of an atom (or molecule), and $f(\mathrm{v}_x, \mathrm{v}_y, \mathrm{v}_z)\mathrm{d}\mathrm{v}_x\mathrm{d}\mathrm{v}_y\mathrm{d}\mathrm{v}_z$ is the probability to find an atom with a velocity v_x, v_y, v_z in the velocity element $\mathrm{d}\mathrm{v}_x\mathrm{d}\mathrm{v}_y\mathrm{d}\mathrm{v}_z$. The integral over the distribution is equal to unity,

$$\int_{-\infty}^{\infty}\int_{-\infty}^{\infty}\int_{-\infty}^{\infty} f\,\mathrm{d}\mathrm{v}_x\mathrm{d}\mathrm{v}_y\mathrm{d}\mathrm{v}_z = 1. \tag{14.3}$$

How large is the probability to find an atom in the velocity interval $\mathrm{v}_z, \mathrm{v}_z + \mathrm{d}\mathrm{v}_z$ (Fig. 14.1a)? It is

$$f(\mathrm{v}_z)\mathrm{d}\mathrm{v}_z = \left(\frac{a}{\pi}\right)^{3/2} \mathrm{e}^{-a\mathrm{v}_z^2}\mathrm{d}\mathrm{v}_z \int_{-\infty}^{\infty} \mathrm{e}^{-a\mathrm{v}_x^2}\mathrm{d}\mathrm{v}_x \int_{-\infty}^{\infty} \mathrm{e}^{-a\mathrm{v}_y^2}\mathrm{d}\mathrm{v}_y, \tag{14.4}$$

where $a = m/2kT$ is an abbreviation. It follows, with

$$\int_{-\infty}^{\infty} \mathrm{e}^{-a\mathrm{v}_x^2}\mathrm{d}\mathrm{v}_x = (\pi a)^{-1/2}, \tag{14.5}$$

that

$$f(\mathrm{v}_z) = \sqrt{\frac{m}{2\pi kT}} \exp\left(-\frac{m}{2kT}\mathrm{v}_z^2\right). \tag{14.6}$$

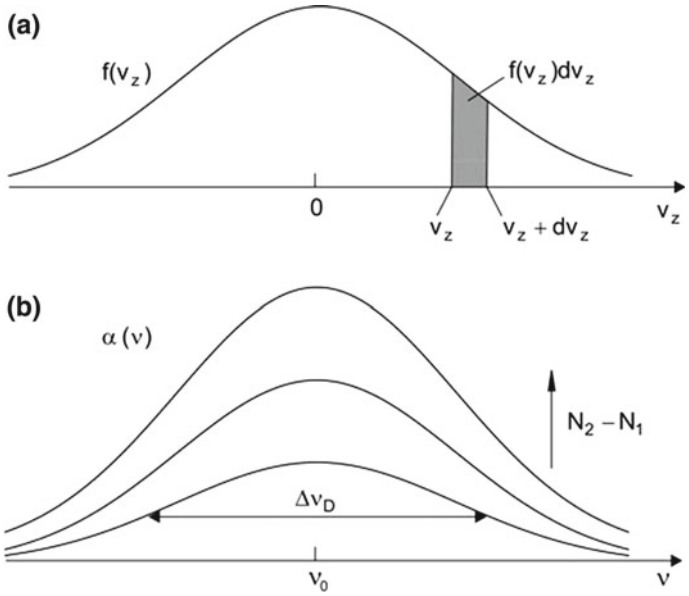

Fig. 14.1 Doppler broadening. **a** Maxwellian velocity distribution. **b** Gain coefficient of a medium with a Doppler broadened line

How large is the probability $g(\nu)\mathrm{d}\nu$ of a transition in the frequency interval ν, $\nu + \mathrm{d}\nu$? The answer is

$$g(\nu)\mathrm{d}\nu = f(\mathrm{v}_z)\mathrm{dv}_z. \tag{14.7}$$

With

$$\mathrm{dv}_z = \frac{c}{\nu_0}\,\mathrm{d}\nu, \tag{14.8}$$

we obtain

$$g(\nu) = \frac{2}{\Delta\nu_\mathrm{D}}\left(\frac{\ln 2}{\pi}\right)^{1/2} \exp\left[-\ln 2\,\frac{(\nu-\nu_0)^2}{(\Delta\nu_\mathrm{D}/2)^2}\right], \tag{14.9}$$

where

$$\Delta\nu_\mathrm{D} = 2\nu_0\sqrt{\frac{2kT\ln 2}{mc^2}} \tag{14.10}$$

is the *Doppler linewidth*. It depends on the temperature and the atomic mass of the atoms and is independent of the gas pressure. The Doppler broadening leads to a Gaussian line. The Doppler broadening is an inhomogeneous broadening mechanism because atoms of different velocities have emission lines (and absorption lines) at different frequencies.

The gain coefficient $\alpha(\nu)$ of an active medium with a Doppler broadened transition is proportional to the population difference $N_2 - N_1$ (Fig. 14.1b). The halfwidth of the gain curve is independent of $N_2 - N_1$.

Example Helium–neon laser; $\lambda = 633\,\mathrm{nm}$; $m_\mathrm{Ne} = 20\,m_\mathrm{p}$; m_p = proton mass; $k = 1.38 \times 10^{-23}\,\mathrm{J\,K^{-1}}$; $\Delta\nu_\mathrm{D} = 1.5 \times 10^9\,\mathrm{Hz}$.

14.2 Collision Broadening

According to a classical description of *collision broadening* (= pressure broadening) in gases, a collision of an excited atom with another (nonexcited) atom changes the phase of the sinusoidal oscillation of the excited atom. Therefore, collisions change the phase of radiation emitted by the atom (Fig. 14.2a); *see* also Sect. 4.11. The time τ_c between two collisions is a dephasing time. Between two collisions, an electron of the excited atom performs, in the picture of the classical oscillator model, (Sect. 4.8), an oscillation with the transition frequency.

A Fourier analysis of the electric field emitted by the atom leads to a Lorentzian line

$$g_\mathrm{L,res}(\nu) = \frac{\Delta\nu_c}{2\pi}\,\frac{1}{(\nu_0-\nu)^2 + \Delta\nu_c^2/4}. \tag{14.11}$$

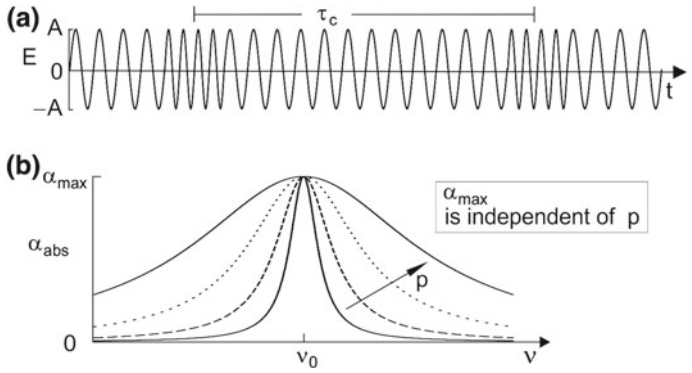

Fig. 14.2 Collision broadening. **a** Collision time. **b** Absorption coefficient

The linewidth is equal to

$$\Delta\nu_c = \frac{1}{\pi\,\tau_c}. \tag{14.12}$$

The theory of collision broadening provides, in accordance with experimental results, a relation between linewidth and collision time,

$$\Delta\nu_c = \sqrt{\frac{8}{\pi}}\,\frac{\sigma_c^2}{\sqrt{mkT}} \times p = K \times p. \tag{14.13}$$

The linewidth is proportional to the pressure. K is a characteristic constant of a gas, σ_c is the cross section of collisions, m the mass of the gas molecules (or atoms) and p the gas pressure. At room temperature, $K \sim 1\,\mathrm{GHz}/p$, where p is measured in units of bar; K has values between 0.3 and $2.5\,\mathrm{GHz}/p$, depending on the atoms or molecules.

The collision broadening corresponds to a homogeneous broadening mechanism because all atoms are submitted to collisions. The absorption coefficient of radiation interacting with a pressure broadened transition is equal to

$$\alpha_{\mathrm{abs}}(\nu) = (h\nu/c)B_{12}g_L(\nu)N_1. \tag{14.14}$$

N_1 is the (number) density of molecules (atoms). The density is proportional to pressure. The maximum of the lineshape function is inversely proportional to pressure. Therefore, the absorption coefficient at line center is independent of pressure while the linewidth increases linearly with pressure (Fig. 14.2b).

The gain coefficient of an active medium consisting of molecules with a collision broadened line is equal to

$$\alpha(\nu) = (h\nu/c)B_{12}g_L(\nu) \times (N_2 - N_1). \tag{14.15}$$

Example CO_2 laser operated at large gas pressure (Sect. 14.8).

14.3 Helium–Neon Laser

The helium–neon laser belongs, besides the ruby laser, to the two first lasers and is still in use. In the helium–neon laser, Ne atoms are excited into s states (Fig. 14.3a). Laser transitions are s → p transitions. The helium–neon laser is a three-level laser type. Accidentally, the second lowest excited state of a helium atom (2^1S state) has almost the same energy as the 5s state of Ne. This coincidence allows for a selective excitation of the 5s state of Ne:

- In a gas discharge, electrons excite helium atoms; the excited helium atoms have very long lifetimes.
- Atomic collisions between excited He and Ne atoms lead to a transfer of excitation energy from He to Ne atoms.
- Stimulated 5s → 3p transitions result in generation of laser radiation of a wavelength of 633 nm.
- The 3p levels are depopulated by spontaneous emission of radiation (wavelength near 450 nm) by 3p → 3s transitions. The 3s state has a very long lifetime. Relaxation is possible via collisions of the neon atoms in the 3s state with the wall of the tube that contains the gas; it is a process of nonradiative relaxation. To obtain a sufficiently fast relaxation, a narrow gas tube is favorable.
- The lifetime of the 5s state is about 100 ns and the lifetime of the 3p state about 10 ns.
- Stimulated 5s → 4p transitions lead to generation of laser radiation of a wavelength of 3.4 μm.

The lowest excited state level of He (2^3S state) almost coincides with the 4s level of neon; the energy difference (∼40 meV) is equal to $\sim 2kT$. Helium atoms, excited by electron collisions to their lowest excited state, transfer the excitation energy to neon atoms resulting in a population of the 4s level of neon. Stimulated 4s → 3p transitions lead to generation of laser radiation at a wavelength of 1.15 μm.

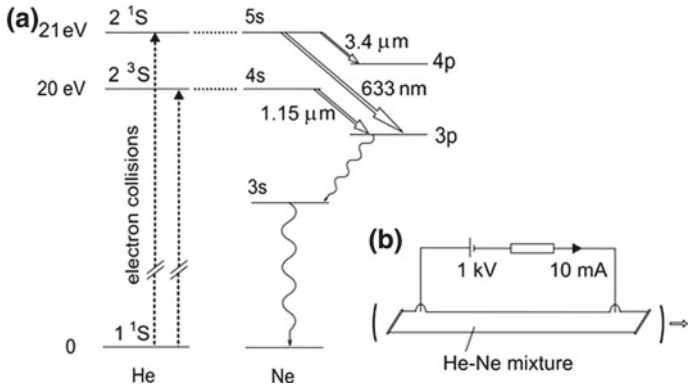

Fig. 14.3 Helium–neon laser. **a** Principle. **b** Arrangement

The helium–neon laser (Fig. 14.3b) contains a gas mixture of helium and neon (ratio 5:1; pressure ∼5 mbar) in a glass tube (typical length 0.5 m; diameter 1–2 mm). Brewster windows close the tube. Radiation of the appropriate polarization passes the windows without reflection loss (*see* Fig. 2.16). A gas discharge (voltage ∼2 kV; current ∼10 mA) leads to a laser output power (∼1 mW at 633 nm), which corresponds to an efficiency of the order of 0.01%. There are different reasons that the efficiency is small: the quantum efficiency is small and the pump process is not very efficient in the helium–neon gas. The laser resonator (especially the coating on the dielectric reflectors) determines the wavelength of a helium–neon laser.

Table 14.1 shows data of different helium–neon lasers; $\Delta\nu_g$ is the gain bandwidth.

The electronic configuration of Ne is $1s^2 2s^2 2p^6$. Excited states have the configurations $1s^2 2s^2 2p^5$—3s, 3p, 4s etc. The 3s, 3p, ... levels are split because of the interaction of an excited electron with the hole in the 2p shell (spin-orbit interaction). The s levels are split into 4 sublevels and the p levels into 10 sublevels. Due to the level splitting, a large number of transitions are available as laser transitions—about a hundred laser lines (many of them in the infrared and far infrared) are known. The first helium–neon laser operated in the infrared (wavelength 1.15 μm).

Figure 14.4 indicates a possible labeling of the energy levels of Ne. The $3s_2$ sublevel is the highest 3s level; the sublevels have the numbers 2 ... 5. The highest 2p

Table 14.1 Helium–Neon lasers

λ	Transition	$\Delta\nu_g$ (GHz)	α (m^{-1})	Power (mW)
543 nm	$3s_2 \rightarrow 2p_{10}$	1.75	0.005	1
594 nm	$3s_2 \rightarrow 2p_8$	1.60	0.005	1
612 nm	$3s_2 \rightarrow 2p_6$	1.55	0.017	1
633 nm	$3s_2 \rightarrow 2p_4$	1.50	0.1	1–10
1.15 μm	$2s_2 \rightarrow 2p_4$	0.83		1
1.52 μm	$2s_2 \rightarrow 2p_1$	0.63		1
3.39 μm	$3s_2 \rightarrow 3p_4$	0.28	100	10

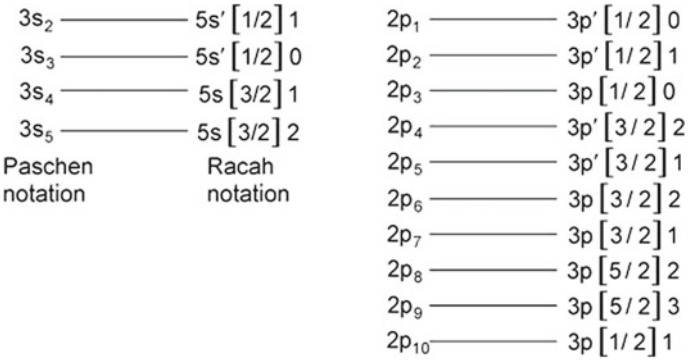

Fig. 14.4 Sublevels of Ne

sublevel is $2p_1$ and the lowest 2p level is $2p_{10}$. In this notation (*Paschen* notation), the Ne^+ core is considered as an effective potential and the states of the additional electron are 1s, 2s, 2p, etc. An alternative, more detailed analysis uses the *Racah* notation: an excited neon atom has the configuration $1s^2 2s^2 2p^5$ plus an additional state with one electron (the outer electron). In the Racah notation, an energy level (for instance a 5s sublevel) is characterized by 5s[K]J or 5s′[K]J, where the symbols indicate the following:

- 5s or 5s′; configuration of the outer electron.
- K; quantum number of the sum of the total angular momentum J_c (quantum number j) of the core electrons and the orbital momentum L (quantum number l) of the outer electron.
- $J = K \pm \frac{1}{2}$, where $\frac{1}{2}$ is the quantum number of the spin of the outer electron.

The coupling leads to 4 sublevels of s states (Fig. 14.4); s is attributed to a state with $K = 3/2$ and s′ to a state with $K = 1/2$. A p state has 10 sublevels; 3p[K] configurations ($j = 3/2$) are possible with $K = 1/2$, 3/2 and 5/2 while 3p′[K] configurations are possible with $K = 1/2$ and 3/2. The coupling corresponds to intermediate coupling ($j - l$ coupling). The energy levels (energy values, lifetimes, and assignment to appropriate quantum states) have been studied long before the arrival of the laser; for discussions of Ne levels used in lasers, *see* [116–118].

Applications. The helium–neon laser generates monochromatic radiation with a small beam divergence. The laser serves for various applications (e.g., holography), which need a high coherence and low beam divergence.

14.4 Metal Vapor Laser

A metal vapor laser operates with copper, gold, lead, or cadmium vapor. In the copper vapor laser (Fig. 14.5), Cu atoms are excited by electron collisions from the ground state $3d^{10}4s$ to the $3d^{10}4p$ state, giving rise to stimulated transitions to $3d^9 4s^2$ states.

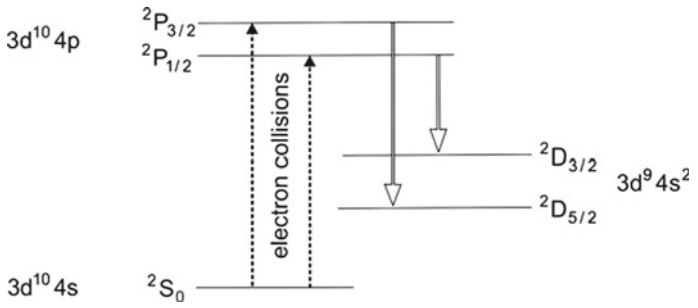

Fig. 14.5 Copper vapor laser

The level splitting is due to spin–orbit interaction. The levels are labeled according to the LS coupling (Russel-Saunders coupling); a level $^{2S+1}L_J$ corresponds to a state with the quantum number L of the orbital momentum, the quantum number S of the spin, and the quantum number $J = L + S$ of the total momentum. $2S + 1$ is the spin multiplicity and the S, P, D states correspond to states with $L = 0, 1, 2$.

A copper vapor laser consists of a ceramic tube (with Brewster windows) in the laser resonator. The tube contains a little piece of metallic copper. The laser oscillation depends very sensitively on the gas pressure and therefore on the temperature. There is only a narrow temperature window (1,500 °C ± 20 °C) in which the laser operates. Population inversion is produced by electric pulses (duration 20 ns; pulse energy 10 mJ; repetition rate 3 kHz). An electric pulse causes a pulsed discharge and excitation of copper atoms via electron collisions. The lifetime of the upper laser level is smaller than the lifetime of the lower laser level. Therefore, continuous oscillation is not possible; the laser is a *self-terminating laser*.

The copper vapor laser has a large gain coefficient (7 m^{-1}), and it has an excellent beam quality because of a large diameter of the active medium and of the resonator. The efficiency of conversion of electric pump energy to energy of laser radiation is about 1%.

Copper vapor lasers generate radiation at the wavelengths 510 and 578 nm and gold vapor lasers at 628 and 312 nm.

Applications lie in medicine, particularly in the detection and destruction of tumors by the photodynamic therapy. Today, metal vapor lasers are competing with semiconductor lasers.

14.5 Argon Ion Laser

In the argon ion laser (Fig. 14.6), subsequent electron collisions lead to ionization of argon atoms and to excitation of argon ions. The electron configurations are the following:

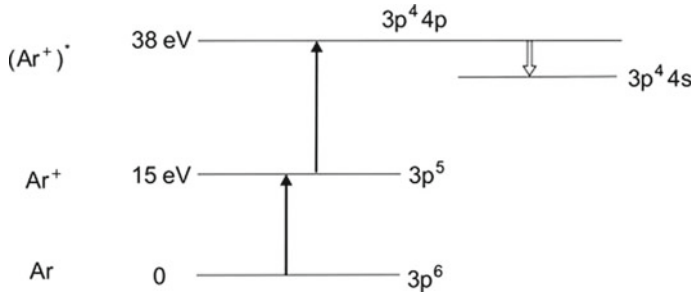

Fig. 14.6 Argon ion laser

- Ar $1s^2\ 2p^6\ 3s^2\ 3p^6$; argon.
- Ar^+ $1s^2\ 2p^6\ 3s^2\ 3p^5$; argon ion.
- $(Ar^+)^*$ $1s^2\ 2p^6\ 3s^2\ 3p^4\ 4p$; excited argon ion.

Different $4p \rightarrow 4s$ transitions between the $3p^4 4p$ and $3p^4 4s$ levels (split due to spin–orbit interaction) give rise to cw laser emission in the blue and green, with strong emission lines at 488 and 514.5 nm.

A gas discharge in a ceramic tube (diameter 1–2 mm; length 1 m; cooled with water) containing the argon gas (pressure 0.1 mbar) pumps the argon ion laser. Because of the twofold excitation, the efficiency of the argon ion laser is proportional to the square of the current density in the gas discharge. At a high electric power (current 10 A; voltage 5 kV), the output power is large (20 W). The efficiency of the laser is small ($\leq 0.1\%$).

The krypton ion laser operates in the same way as the argon ion laser; it emits radiation at other wavelengths (between 406 and 676 nm). An important application of the argon and the krypton ion lasers is the optical pumping of other lasers, especially of the titanium–sapphire laser (and before this laser existed, the optical pumping of dye lasers). Today, semiconductor lasers serve as pump lasers.

14.6 Excimer Laser

We now treat an important industrial laser. The *excimer laser* makes use of the KrF excimer or of other excimers. The following processes occur in a KrF excimer laser (Fig. 14.7).

- A gas discharge in a mixture of krypton and fluorine gas produces $(KrF)^*$ molecules, i.e., KrF molecules in an excited electronic state. The lifetime of the excited state is of the order of 10^{-9} s.
- Stimulated transitions take place to nonbonding KrF states. After a transition, the Kr atom and the F atom repel each other and separate spatially. Therefore, the lower laser level has a shorter lifetime than the upper laser level. During an optical transition in a KrF excimer, the nuclear distance R_{Kr-F} between the nucleus of Kr and the nucleus of F does not change (Franck–Condon principle)—the transition corresponds to a vertical line in the energy-nuclear distance diagram.

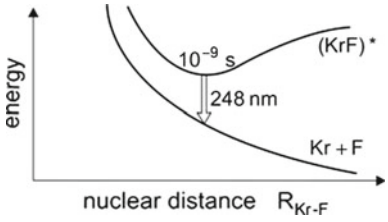

Fig. 14.7 KrF excimer laser

- The excitation occurs by electron collisions with Kr and by a chemical reaction, respectively, $Kr + e^- \rightarrow Kr^* + e^-$ and $Kr^* + F_2 \rightarrow (KrF)^* + F$:

An excimer (excited dimer) is a molecule with two equal atoms, which undergo chemical bonding in the excited state but not in the ground state.
Examples of excimers: Ar_2^* (emission at 126 nm); Kr_2^* (146 nm); Xe_2^* (172 nm). An exciplex (excited state complex) is denoted as excimer too.
Examples of exciplexes (excimers) and laser lines: ArF (193 nm); KrF (248 nm); XeCl (308 nm); XeF (351 nm); KrBr (206 nm); ArBr (161 nm); NeF (108 nm).

The excimer laser is a TEA laser (transversely excited atmospheric laser). We will describe a TEA laser arrangement in connection with the CO_2 laser (Sect. 14.8). The laser gas of a krypton fluoride excimer laser has the composition: He (= buffer gas, pressure ~1 bar); Kr (10%); and F_2 (0.1%). At a large pump power density (200 MW per liter gas volume), the gain is about 10% per cm (gain coefficient $\alpha = 10\,\mathrm{m}^{-1}$).

Data of an excimer laser: pumping by electric discharge pulses (voltage ~1 MV, current 10 kA, pulse duration 30 ns, electric energy per pulse 100 J); laser pulse energy 1 J; efficiency 1%; repetition rate 1–50 Hz.

Applications of the excimer laser are: labelling (of semiconductor chips, glasses, polymers, etc.) during mass production; structuring of materials by means of UV lithography—in 2011, semiconductor structures of lateral size of 45 nm are prepared by the use of the ArF laser (wavelength 193 nm).

14.7 Nitrogen Laser

The nitrogen laser is a prototype of a vibronic laser (Fig. 14.8). The electronic energy depends on the distance R_{N-N} between the nitrogen nuclei. A vibronic energy level of N_2 has electronic and vibrational energy,

$$E_{\mathrm{n,v}} = E_{\mathrm{n}} + \left(\mathrm{v} + \frac{1}{2}\right) h\nu_{\mathrm{vib}}. \tag{14.16}$$

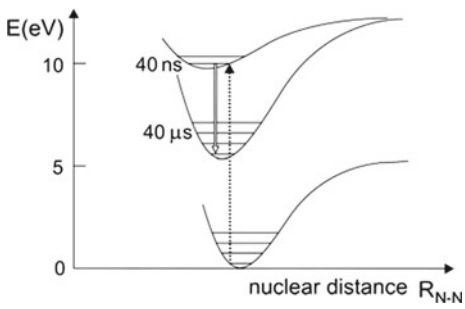

Fig. 14.8 Nitrogen laser

E_n is the electronic energy in the nth state; n = 1, ground state; n = 2, 3, ..., excited states; $(v + 1/2)h\nu_{vib}$ is the vibrational energy; v = 0, 1, 2, ... are the vibrational quantum numbers; and ν_{vib} (= 70.8 THz) is the vibrational frequency. Electron collisions in a gas discharge excite N_2 molecules to vibronic states belonging to the n = 3 electronic state. Stimulated transitions to vibronic levels of the n = 2 electronic level (energies $E_{2,v}$) produce laser radiation in the near UV (near 337 nm). The lifetime (40 ns) of the upper laser level is shorter than the lifetime of the lower laser level. Therefore, continuous operation is not possible; the laser is a self-terminating laser. Suitable for pumping are very short gas discharge pulses (duration 1 ns). Optical transitions obey the Franck–Condon principle.

14.8 CO_2 Laser

The CO_2 laser is of great importance:

- It has a high efficiency (10–50%) for conversion of electrical power to power of laser radiation.
- Different ways of operation are possible; in particular, cw operation, pulsed operation, and TEA laser operation.
- The cw CO_2 laser generates cw radiation of a large power (100 W at a length of the active medium of about 1 m, and up to 1,000 W or even more at very large length of the active medium).
- The TEA (transversely excited atmospheric) CO_2 laser produces pulses (duration ~100 ns) of high peak power (100 kW).

Applications of CO_2 lasers concern material processing (cutting, welding, hardening of metal surfaces, shock hardening at power densities of 10^9 W/cm^2) and medicine.

The CO_2 laser (Fig. 14.9a) makes use of vibrational-rotational levels,

$$E = E_{vib}(v_1, v_2, v_3) + E_{rot}(J). \tag{14.17}$$

E_{vib} is the vibrational energy and E_{rot} the rotational energy (J = quantum number of the rotation). The vibrational energy is

$$E_{vib} = \left(v_1 + \frac{1}{2}\right) h\nu_1 + \left(v_2 + \frac{1}{2}\right) h\nu_2 + \left(v_3 + \frac{1}{2}\right) h\nu_3, \tag{14.18}$$

where the oscillation frequency ν_1 (= 41.6 THz) corresponds to the *symmetric valence vibration*, ν_2 (=20.0 THz) to the *bending vibration*, and ν_3 (=70.5 THz) to the *antisymmetric valence vibration* (Fig. 14.9b); v_1, v_2, and v_3 are the vibrational quantum numbers; $v_1 = 0, 1, 2, \ldots$; $v_2 = 0, 1, 2, \ldots$; $v_3 = 0, 1, 2, \ldots$. We denote a state with the quantum numbers v_1, v_2, and v_3 as $v_1v_2v_3$ state.

Electron collisions in a gas discharge can excite CO_2 molecules. More efficient is the indirect excitation. Electron collisions produce excited N_2 molecules

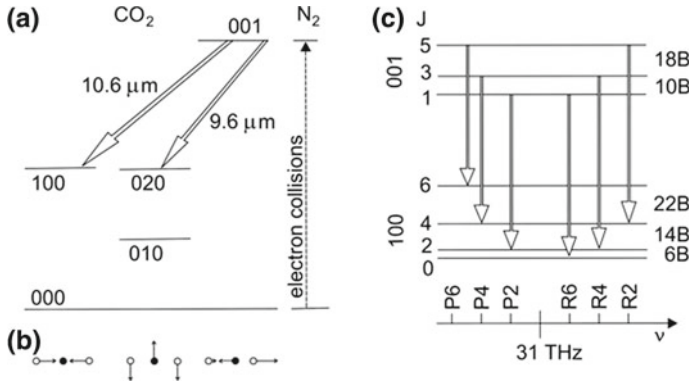

Fig. 14.9 CO_2 laser. **a** Vibrational levels of CO_2 and N_2. **b** Vibrations of the CO_2 molecule. **c** Vibrational-rotational transitions in CO_2

(in the lowest vibrational state); an excited N_2 molecule in the lowest vibrational state has a very large lifetime. Energy transfer processes by collisions between excited N_2 molecules and nonexcited CO_2 molecules lead to population of the 001 state of CO_2 molecules. This state has a very long lifetime (∼4 s) with respect to spontaneous emission of radiation that is due to 001 → 100 and 001 → 100 transitions. There are two groups of laser transitions corresponding to two wavelength regions:

- 10.6 μm; transitions 001 → 100; frequencies near 28 THz.
- 9.6 μm; transitions 001 → 020; frequencies near 31 THz.

The transitions between different types of vibrations are allowed due to the anharmonicity of the vibrations. The depopulation of the lower states occurs by collisions of the molecules with walls (nonradiative relaxation). A vibrational transition in a CO_2 molecule is associated with a change of the rotational energy (Fig. 14.9c), where one of the selection rules

$$\Delta J = \pm 1 \tag{14.19}$$

must be fulfilled. The selection rule $\Delta J = +1$ corresponds to laser lines in the P branch and the selection rule $\Delta J = -1$ in laser lines in the R branch. The rotational energy is (approximately)

$$E_{\text{rot}} = BJ(J+1); \quad B = \frac{\hbar^2}{2\Theta}. \tag{14.20}$$

B (∼15 GHz times h) is the rotational constant that is a measure of the rotational energy and Θ is the moment of inertia of a CO_2 molecule; each J state is $2J + 1$ fold degenerate.

Not all rotational quantum numbers lead to allowed states. The CO_2 molecule is a Boson (more exactly, the $^{12}C^{16}O_2$ molecule). Interchange of the two O atoms must leave the total wave function of the molecule unchanged—the wave function must

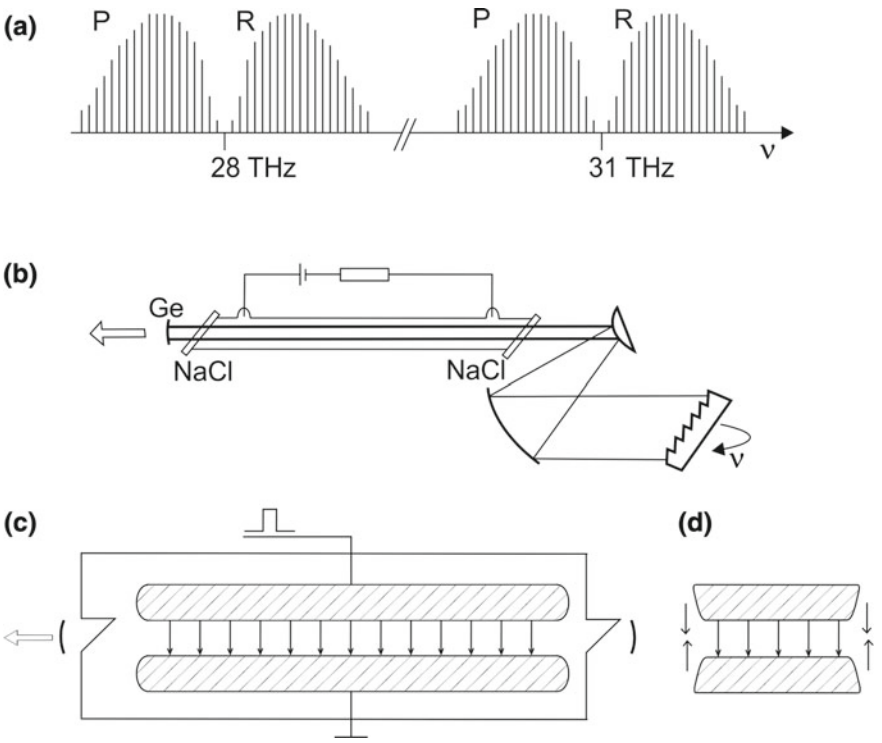

Fig. 14.10 CO_2 laser. **a** Laser lines. **b** Continuous wave CO_2 laser. **c** TEA (*transversely excited atmospheric*) CO_2 laser. **d** Profile of the electrodes of a TEA laser, together with discharge needles causing UV pre-ionization at the arrival of an electric pulse

be an even function. The electronic wave function of the electronic ground state of the molecule is even as well as the wave function of the nuclei (the nuclear spins of ^{12}C and of ^{16}O are zero). It follows: J is odd for an antisymmetric vibration, J is even for a symmetric vibration.

The frequency distance between two neighboring lines is $2 \times 2B/h = 4B/h$. Because of centrifugal distortion, the distance between two neighboring lines is not exactly $4B/h$ but depends on the vibrational quantum number and on the rotational quantum number. About twenty discrete laser lines belong to each of the four branches (Fig. 14.10a). The distance between next—near lines is ~60 GHz, or less because of the centrifugal distortion.

A gas discharge pumps the cw CO_2 laser (Fig. 14.10b). The gas, a mixture of CO_2, N_2, and He (at a ratio of about 1:1:8), can have a pressure of about 1 mbar. The glass tube (diameter 1 cm) that contains the laser gas is closed by Brewster windows (NaCl crystal plates). The spherical output coupling mirror consists of crystalline germanium. The outer side of the germanium mirror is covered with an antireflecting dielectric multilayer coating. Thus, standing waves in the output coupling mirror are avoided. The other surface, covered with another dielectric multilayer coating, has a reflectivity (~95%) that is appropriate to reach optimum output coupling.

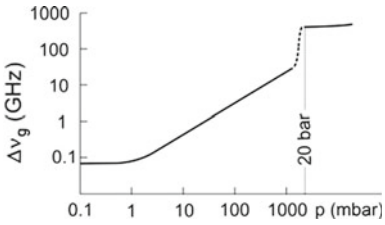

Fig. 14.11 Broadening of vibrational-rotational lines of CO_2

An echelette grating in the expanded beam is the reflector of the laser resonator. By rotating the echelette grating, the laser resonator is adjusted to different lines.

In the TEA CO_2 laser (Fig. 14.10c), the direction of the gas discharge (at a pressure of ≈1 bar) is transverse to the laser beam. Two Brewster windows (NaCl plates) are closing a box containing the laser gas. The resonator mirrors are outside the box. A power supply charges a Marx generator (a capacitor bank with many capacitors in parallel and in series). An electric switch starts the discharge leading to high-power electric pulse (voltage 100 kV; current 100 A; duration 20 ns). The electric pulse, guided to one of the electrodes, causes a transverse discharge between the electrodes. The electrodes (distance 1 cm, length 40 cm) of the TEA laser (Fig. 14.10d) have a special profile (Rogowski profile) providing a homogeneous discharge. Arc discharges between the tips of metal needles initiate the discharge. The arc discharges produce UV radiation, which causes pre-ionization of molecules in the volume between the main electrodes. A gas discharge between pairs of needles, arranged along the electrodes (on both sides of the discharge volume), occurs when a high voltage pulse arrives at the electrodes. The TEA laser is a multi-mode laser; a single pulse consists of radiation at several modes (longitudinal and transverse modes).

At small gas pressure, Doppler broadening of the vibrational-rotational lines of CO_2 determines the width of the lines (Fig. 14.11). Collision broadening dominates at pressures between 5 mbar and about 1,000 mbar; in this pressure range, the gain bandwidth increases proportionally to pressure. At still higher pressure, the vibrational-rotational lines overlap partly and above a pressure of 20 bar the single vibrational-rotational lines overlap completely. Then the gain profile of each of the four branches is continuous and has a width of about 500 GHz. A mode locked high-pressure CO_2 laser operating on one of the four branches produces picosecond pulses (duration ∼1 ps) consisting of radiation around a frequency of 30 THz.

14.9 Other Gas Discharge Lasers and Optically Pumped Far Infrared Lasers

Beside CO_2 lasers, there are other infrared and far infrared gas discharge lasers (Fig. 14.12). Laser oscillation is due to stimulated emission of radiation by transitions between vibrational-rotational levels (CO laser) or between rotational levels (D_2O and HCN lasers) in the vibrational ground state or an excited vibrational state.

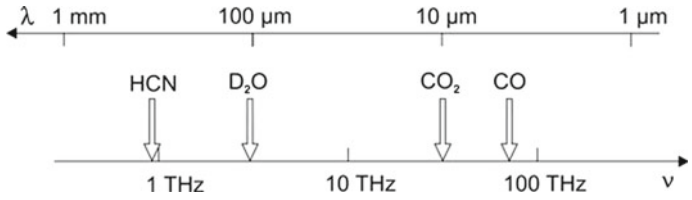

Fig. 14.12 Gas discharge lasers in the 1–100 THz range (*far infrared range*)

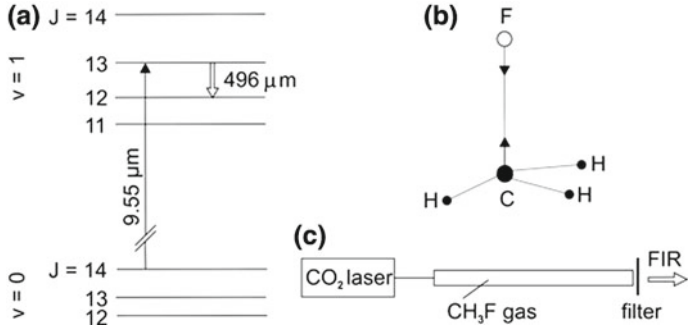

Fig. 14.13 Optically pumped CH_3F laser. **a** Principle. **b** CH_3F vibration. **c** Arrangement

The CO_2 laser is suitable for optical pumping of other gas lasers. Lasers operated with gases of CH_3F, D_2O, and alcohol molecules (and many other organic molecules) emit far infrared radiation at a large number of wavelengths.

Figure 14.13a shows an example of an optically pumped gas laser. Radiation of a CO_2 laser excites CH_3F from the vibrational ground state to an excited vibrational state. The vibration of the CH_3F molecule corresponds to a vibration of CH_3 against F (Fig. 14.13b). Stimulated rotational transitions ($J = 13 \rightarrow J = 12$) generate far infrared laser radiation (wavelength 496 µm, frequency near 605 GHz). A lens focuses the radiation of a CO_2 laser into a glass tube that contains the gas (Fig. 14.13c). A filter absorbs CO_2 laser radiation passing the tube.

Optical pumping is also possible if the CO_2 laser line and the absorption line of CH_3F do not completely coincide. Then stimulated Raman scattering (Sect. 35.8) results in generation of far infrared radiation. A variation of the CO_2 laser frequency leads to a variation of the frequency of the far infrared laser. The tuning range, however, is small (about 0.1% relative to a far infrared laser line).

The optically pumped gas lasers emit, depending on the gas and the wavelength of the CO_2 pump laser, radiation at a very large number of frequencies (about ten thousand laser lines have been reported). A gas laser pumped by a TEA laser generates intense far infrared radiation pulses (pulse power about 1 kW [119]).

In comparison with optically pumped cw far infrared gas lasers, quantum cascade lasers (Chap. 29) are becoming important alternatives. In comparison with far infrared

gas lasers optically pumped by TEA CO_2 lasers, free-electron lasers (Chap. 19) produce tunable single mode radiation.

References [1–4, 6, 35, 106–119].

Problems

14.1 Helium–neon laser: line broadening and gain cross section. Show that Doppler broadening is the dominant broadening mechanism for a helium–neon laser operated at 633 nm. Compare the different linewidths that are caused by different effects.

(a) Doppler broadening.
(b) Collision broadening (pressure 0.5 mbar).
(c) Natural line broadening.
(d) Line broadening due to the finite lifetime of the lower laser level (3p).
(e) And estimate the gain cross section σ_{21}.

14.2 Helium–neon laser: threshold condition, output power and oscillation onset time. A helium–neon laser is characterized by: length of the active medium L = 0.5 m; cross section $a_1 a_2 = 4\,\text{mm}^2$; reflectivity of the output coupling mirror $R = 0.98$; reflectivity of the reflector $R = 0.998$. Determine the following quantities:

(a) Threshold population difference per m^3.
(b) Absolute value of the threshold population difference.
(c) Output power at a pump rate that is 10 times stronger than at threshold.
(d) Oscillation onset time.

14.3 Doppler effect in the helium-neon laser and Lamb dip.

(a) Calculate the frequency difference of the emission line at 633 nm for a neon atom that moves with a velocity of 500 m/s toward an observer and of an atom that moves with the same velocity away from the observer.
(b) In which velocity range do the emission lines overlap?
(c) Discuss the consequence for the gain in a helium–neon laser: the gain shows a minimum at the line center of the gain curve (= Lamb dip, according to W. Lamb).

14.4 CO_2 laser (length $L = 1$ m; cross-sectional area $a_1 a_2 = 1\,\text{cm}^2$; reflectivity of the output coupling mirror $R = 0.7$; lifetime of the upper laser level with respect to spontaneous emission of radiation by $2 \rightarrow 1$ transitions, $\tau^*_{\text{rel}} = 4$s; gas pressure 10 mbar).

(a) Calculate: Doppler linewidth; gain cross section; threshold condition; pump rate (relative to the threshold pump rate) that is necessary to obtain an output power $P_{\text{out}} = 60$ W.

(b) Discuss the onset of laser oscillation taking into account that the upper laser level has a long lifetime with respect to spontaneous emission and that there are many rotational levels belonging to the excited state.
(c) Estimate the maximum gain coefficient of an excited CO_2 gas and the corresponding small-signal gain factor of radiation in a cw CO_2 laser. [*Hint*: the maximum gain coefficient is determined by the density of CO_2 molecules that are available in a gas at low pressure.]
(d) Show that the gain coefficient of an excited CO_2 gas in a TEA laser or in a high pressure CO_2 laser (pressure 20 bar) is about the same as in a cw laser at a gas pressure of 10 mbar. Why is the pulse power of a TEA laser or of a high pressure laser much larger than the power of the cw laser? Estimate the radiation energy of a pulse within a TEA laser.
(e) Estimate the oscillation onset time of a TEA laser.

14.5 Optical radar.
Determine the frequency difference between the frequency of radiation emitted by a helium–neon laser and the frequency of radiation reflected by a car traveling at a velocity of 60 km per hour.

14.6 CO molecule.

(a) Estimate the isotope shift of the vibrational frequency of CO (frequency $\tilde{\nu} = 2{,}170\,\mathrm{cm}^{-1}$) if ^{16}O is replaced by ^{18}O.
(b) Next-near lines that are due to transitions between vibrational-rotational levels have a frequency separation of $3.86\,\mathrm{cm}^{-1}$. Determine the rotational constant $\tilde{B} = B/(hc)$. Which of the rotational levels has the highest occupancy at room temperature?

14.7 Rotational levels at thermal equilibrium.

(a) Which of the J levels of a CO_2 molecule in the vibrational ground state has the largest occupancy in a gas at room temperature?
(b) Determine the excitation energy and the occupancy of the $v = 0$, $J = 1$ state of a nitrogen molecule (N–N distance = 0.1 nm) in a gas at room temperature.

14.8 Estimate the density of neon atoms, the density of excited neon atoms, and the corresponding absolute numbers of nonexcited and excited neon atoms in a helium–neon laser.

14.9 Explain the nomenclature used to characterize: (a) the two lowest excited states of He; (b) the ground state and the four lowest excited states of Cu; (c) the states of Ar, Ar^+ and $(Ar^+)^\star$.

14.10 Spatial hole burning and diffusion of excited molecules in a CO_2 laser.
On the one hand, the excitation of CO_2 molecules in a gas discharge occurs homogeneously in the gas discharge tube. On the other hand, the amplitude of the standing wave field in the laser resonator shows a $\sin z$ dependence along the resonator

axis. The stimulated emission is therefore spatially inhomogeneous. Show that—nevertheless—all excited CO_2 molecules can contribute to stimulated emission. Study the problem in case of a cw CO_2 laser (length 0.7 m; gas pressure 5 mbar; ratio He:Ne:CO_2 = 6:1:1; spontaneous lifetime of an excited CO_2 molecule $\tau_{sp} \sim$ 5s; reflectivity of the output mirror $R = 0.95$; efficiency of conversion of pump power to power of laser radiation $\sim 20\%$).

(a) Determine the density of CO_2 molecules.
(b) Determine the density of excited CO_2 molecules.
(c) Estimate the diffusion constant $D = \bar{v}\lambda_m/3$, where $\bar{v}$ is an average velocity and λ_m ($\sim 100\,\mu$m) the mean free path of a CO_2 molecule with respect to a collision with another atom or molecule in the gas mixture of a CO_2 laser.
(d) Estimate the time τ_{esc} it takes an excited CO_2 molecules to escape from a region of weak field strength to a region of large field strength. [*Hint*: replace the cosine squared field distribution by a rectangular distribution and apply a one-dimensional diffusion equation to describe the dynamics of the local density N_{loc} of excited CO_2 molecules, $dN_{loc}/dt = D d^2N_{loc}/dx^2$.]

14.11 Collision cross sections of molecules in a CO_2 laser. Estimate the cross sections of collisions of CO_2 molecules with other CO_2 molecules, with N_2 molecules and with helium atoms. [*Hint*: Use the hard-sphere approximation of the cross section, $\sigma_c = \pi/4(d_1 + d_2)^2$, where d_1 and d_2 are the diameters of the two colliding molecules; treat the CO_2 molecule as a sphere (diameter 0.4 nm) as well as the N_2 molecule (diameter 0.2 nm).]

14.12 Voigt profile. A Voigt profile is observed when collision and Doppler broadening influence the spectral broadening of an optical transition. Atoms of velocity v have a transition frequency $\nu = \nu_0 + \nu_0 v/c$. The lineshape function describing optical transitions in these atoms with the transition frequency ω_0' is

$$g(\omega_0', \omega) = \frac{\Delta\omega_0}{2\pi} \frac{1}{(\omega_0' - \omega)^2 + \Delta\omega_0^2/4}. \tag{14.21}$$

where $\Delta\omega_0$ is the halfwidth of a transition. The probability of a transition in the frequency interval $\omega_0', \omega_0' + d\omega_0'$ is equal to

$$P(\omega_0')d\omega_0' = \frac{2\sqrt{\ln 2}}{\sqrt{\pi}\,\Delta\omega_c} \exp\left(-\frac{\ln 2(\omega_0' - \omega_0)^2}{\Delta\omega_c^2/4}\right) d\omega_0'. \tag{14.22}$$

where $\Delta\omega_c$ is the halfwidth and ω_0 the center frequency of the Gaussian profile. We obtain the spectral profile of a line by averaging,

$$S(\omega) = \int_0^\infty g(\omega_0', \omega) P(\omega_0') d\omega_0'. \tag{14.23}$$

It follows that

$$S(\omega) = \frac{\Delta\omega_0}{\pi^{3/2}\Delta\omega_c}\int_0^\infty \frac{1}{(\omega_0' - \omega_0)^2 + \Delta\omega_0^2/4}\exp(-\frac{\mathrm{In}2(\omega_0' - \omega_0)^2}{\Delta\omega_c^2/4})\mathrm{d}\omega_0'. \quad (14.24)$$

The equation has to be solved numerically.

(a) Show that the limits of the Voigt profile are the Lorentzian or the Gaussian profile, depending on the ratio of the two halfwidth $\Delta\omega_0$ and $\Delta\omega_c$.
(b) Show that (14.24) is consistent with (7.52).

14.13 Characterize a carbon dioxide laser that operates with $^{12}C^{17}O_2$ or with $^{13}C^{16}O_2$.

14.14 A cw CO_2 laser beam (power 100 W, diameter 10 mm) hits a stone. How long does it take until the stone is glowing? Assume that the hot range has an extension of 1 mm.

14.15 Diffusion.
Describe diffusion of particles in an infinitely long rectangular slab. At $t = 0$, the particles are homogeneously distributed over the cross section at $x = 0$, with the two-dimensional particle density N_0. [*Hint*: Apply the one-dimensional diffusion equation $\partial\rho/\partial t = D\partial^2\rho/\partial x^2$ where ρ is the three-dimensional particle density.]

(a) Show that it has the solution $N_0/(2\sqrt{2Dt})\exp(-x^2/4Dt)$.
(b) Determine the variance and the halfwidth (FWHM) of the distribution.
(c) Choose as an example $N_0 = 10^{22}\,\mathrm{m}^{-2}$ and $D = 10^{-2}\,\mathrm{m}^2\,\mathrm{s}^{-1}$. Determine the halfwidth of the distribution for the time at which the two-dimensional particle density at $x = 0$ decreased to one half of its original value.